JP&M Engineering
Journal of Petroleum and Mining Engineering

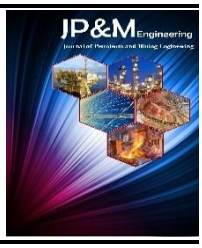

Acoustic Characteristics of Nubia Sandstone at Gebel Abu Hasswa, Gulf of Suez, Egypt

Kassab, M. A.[1], El-Sayed, A. M. A.[2], Abdel-Wahab, S. M.[2], Ali, H. A.[2], Gomaa, M. M.[2,3], El-Sayed, N. A.[1] and Abuhagaza, A. A.[1]*

[1] Exploration Department, Egyptian Petroleum Research Institute(EPRI), Cairo, Egypt.
[2] Geophysics Department, Faculty of Sciences, Ain Shams University, Cairo, Egypt.
[3] Department of Geophysics, University of Miskolc, 3515 Miskolc-Egyetemváros, Hungary.
*Corresponding author e-mail: abeerahmed@epri.sci.eg

Article Info

Received 9 Jan. 2023
Revised 19 Feb. 2023
Accepted 27 Feb. 2023

Keywords

Acoustic velocities; XRD analysis; Petrographical investigations; Nubia sandstone; Petrophysical characteristics

Abstract

On the eastern side of the Gulf of Suez, at Gebel Abu Hasswa, fifty one (51) samples were obtained from different lithofacies of Nubia sandstone units. Acoustic velocity, porosity and permeability have been integrated and confirmed with petrographical investigation. In addition to porosity and permeability analysis, the acoustic wave velocities of dry and wet clastic rock samples are measured to evaluate the influence of diagenesis on reservoir characteristics, which affects the acoustic characteristics of the studied sandstone rocks. Petrographical study determined that all the study samples are mainly quartz arenite facies. The diageneses processes, such as compaction, recrystallization, and cementation, increased compressional and shear wave velocities while decreasing reservoir quality.
The X-Ray Diffraction (XRD) analysis showed that the main mineral that formed samples is quartz mineral, while the minor minerals are calcite, hematite, and kaolinite. From thin sections and XRD results concluded that the samples had been suffered from dissolution process that caused the oversized porosity, in addition to, cementation process with multiple types of cements like silica overgrowth, ferruginous, and calcareous. Depending on the acoustic wave velocities of dry rock samples, the estimated empirical equations can be utilized to predict both the wave velocities (Compressional - Shear wave velocities) of wet rock samples.

Introduction

Nubia sandstone is of special interest for several reasons: (1) the Pharaonic stone monuments in the Upper Egypt were carved from this rock, (2) the Nubian sandstones is considered as the main reservoir of several oil fields in Egypt especially in Gulf of Suez region, (3) the Nubian sandstones also represent the main water aquifer in Egypt especially in western desert, (4) in many localities especially in Sinai the Nubia sandstone intercalated with kaolinite deposits which are of potential economic importance, (5) the Nubian sandstones are the main source of glass sand in Egypt, and (6) the Nubian Sandstone is a variety of sedimentary rock; it consists of continental sandstone with thin beds of marine limestone, and marls which reflects various environmental conditions [1].The huge hydrocarbon production capacity of the Nubian sandstone reservoirs in the Gulf of Suez basin is widely known. They are a sequence of Cambrian - Lower Cretaceous sandstones and shale that overlie the majority of Gulf of Suez area according to [2, 3].

The Middle Jurassic rocks in Khashm El-Galala, western side of Gulf of Suez have been investigated by [4] resulted five microfacies, while acoustic measurements were performed on Middle Jurassic rock samples at Ras El-Abd in both dry and wet conditions and were combined with standard petrophysical parameters to characterize reservoirs [5].

In the presence of ambient conditions, all of the characteristics (Acoustic velocity, porosity and permeability) were determined [6], the acoustic velocities in rocks were governed by a variety of factors including grain density, cementation, porosity, and fluid pressure in pores. The global Jurassic sea-level oscillations were explored by [7], who stated that there was a sea-level drop at the base of the Bajocian and a widespread rise in the Bathonian.

[8] concluded that, the velocity values increase as depth and pressure increase, while dropping as temperature related to pressure increases. Clay content and distribution are important factors in lowering velocities, the clay of pore filling type is considered the most effective type of clay on velocity [9]. [10], concluded that the Nubia samples from Gebel Abu Hasswa are divided into five hydraulic flow

 DOI: 10.21608/jpme.2023.186245.1150

units (HFUs) of various types of rock, with only three electrical -flow units (EFUs). The variation between them could be related to the iron oxide cementations which reduce permeability without a significant reduction in porosity.

In saturated porous rock, the compressional wave velocity is often higher than in dry rock with the exception of materials with poor bulk compressibility and very limited pore volume [11]. The current study's goal is to integrate perographical investigations, XRD analysis, the reservoir properties and acoustic wave velocities of clastic samples (Nubia sandstone) at Gebel Abu Hasswa section to investigate reservoir properties.

The studied samples were collected from outcrops at Gebel Abu Hasswa on the eastern side of the Gulf of Suez to represent various lithofacies of the Nubia sandstone sequence. As shown in Figure 1, the study area is located between Lat. 28° 20' to 28° 40' N and Long. 33° 10' to 33° 30' E.

Geologic Setting

[12, 13] were the first to study Paleozoic rocks in Egypt, Carboniferous sediments were discovered in Sinai and the Eastern Desert. More information about Cambrian sequences in Sinai was provided by [14, 15]. Outcrops from the Devonian period was first shown on the western edge of Gulf Kebir Plateau in south region of Western Desert was reported by [16]. [17] sectioned the Paleozoic Nubia sandstone into the following formations: Araba (Early Cambrian), Naqus (Cambrian), Abu Durba (Lower Carboniferous), Aheimer (Pennsylvanian) and Qiseib (Permo-Triassic) formations. Many stratigraphic sections were measured and many Paleozoic rock units were recognized by [18, 19, 20, 21, 22] Figure (1).

Paleozoic sequence (Cambrian - Permian) with a thickness of several thousand meters have been discovered in the subsurface of the North Western Desert [23, 24, 25, 26, 27, 28]. The Nubia sandstone was classified into 3 sections by [29]. The lithology of Nubia C changes from fine-coarse, conglomerate, soft, and kaolinitic whitish-brown sandstones, the middle Part Nubia B is composed of marine shales, gray - green, silty with sandstones thin interbeds , fine - medium grain size with Permo-Carboniferous trace fossils.

The upper part of Nubia A is composed of fine/coarse fluviatile sandstone, conglomerate, and massive sandstone and sometimes cross-bedding, indicating a south-to-north transport direction, intercalated with fossil- soils formed of mud stones, varicolored, and stratified with root structures. [30] studies the primary structures and the lithofacies of the Nubia Sandstone of Gebel Qabaliat and Gebel Abu Hasswa in south- Sinai. The Lower-Paleozoic rocks of Sinai and Gabal El Zeit, were compared by [1] (Figure 1) and they concluded that the paleo relief of underlying basement surface controls the model of deposition during Cambro-Ordovician Araba Formation.

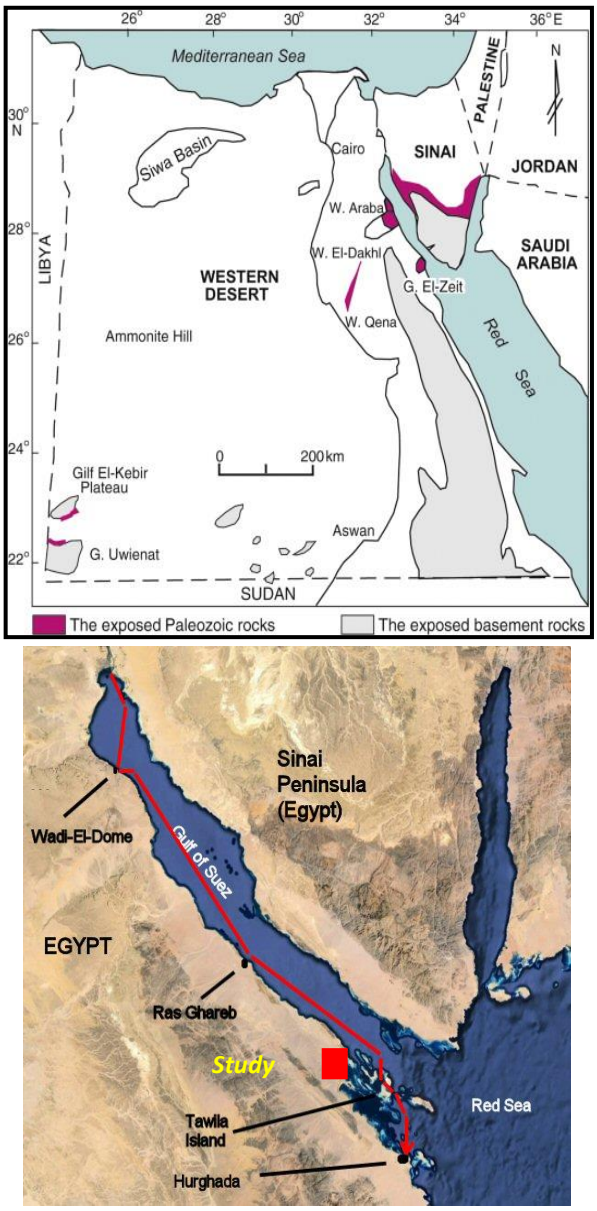

Figure 1: The Location map of study area; map showing the Lower Paleozoic rocks exposed in Egypt (modified after [22].

Materials and methods

Fifty one (51) rock samples were taken from the Nubia sandstone for this study (Table 1). The following methods were undertaken, to carry out the present work: sampling and description of different rock units in sections; using the polarized microscope to detect the mineralogy, diagenesses, as well as its impact on storage capacity of the studied rocks; X-ray diffraction (XRD) of some samples to determine its mineral composition ; laboratory measurements of rock porosity, permeability and densities as well as the laboratory measurements of ultrasonic wave velocities (Vp and Vs) and calculating the relevant elastic parameters like young's modulus, bulk modulus, and rigidity. Each cylindrical sample measured at ambient conditions as dry and wet rocks, which then leads to calculations of the dynamic elastic characteristics of different samples. For the P-Wave the available transducers frequencies were 500 KHz and 100 KHz for S-Wave.

Porosity (Ø)

According to [30], Ø (porosity) was determined by a helium- porosimeter, is equal to vpore (pore spaces volume) divided by Vb (sample's bulk volume):

$$v_{pore} = V_b - V_g \quad (1)$$

$$\emptyset = \frac{v_{pore}}{V_b} \quad (2)$$

Permeability (K)

Porous materials capacity to transfer fluids is defined as permeability (K) in mD. Many factors influence rock permeability (the geometry of rock pores, cementing materials, texture, and grain size). Darcy's equations were used to determine permeability:

$$K = \mu * \frac{u}{\Delta P}, \quad (3)$$

μ is viscosity of air by centipoises, u is the fluid flow rate (cm3 /sec), and ΔP is the pressure difference between inlet and outlet. The mass per unit volume in its normal case is defined rock bulk density as expressed by the following equation:

$$\sigma_b = \frac{W_d}{V_b}, \quad (4)$$

σb is bulk density (g/cm3), Wd is sample's dry mass (g), and Vb is sample's bulk volume (cm3).

Acoustic waves

Samples were measured for velocities (Vp & Vs) in wet and dry cases, and can be estimated from elastic moduli using formulas below:

$$\mathbf{V_p} \left(\frac{\left(\boldsymbol{B} + \frac{\mathbf{4G}}{\mathbf{3}} \right)}{\boldsymbol{\sigma}} \right)^{\frac{1}{2}} \quad (\mathbf{5})$$

$$\boldsymbol{V_s} = \left(\frac{\boldsymbol{G}}{\boldsymbol{\sigma}} \right)^{\frac{1}{2}} \quad (\mathbf{6})$$

B is bulk modulus, G is shear modulus and σ is density. Many authors have written about seismic wave velocities in all reservoirs [31, 32, 33, 34].

Voigt-Reuss model

Seismic analysis for porosity and Litho-facies relies heavily on rock physics models that link velocity, porosity, and mineralogy. The velocity-porosity model [35, 36, 37] (Figure 2a) combines the friable and cemented sand models, with a constant cement value in the sorting trend.

Because elastic moduli are the controlling key for acoustic wave propagation, the lithology of each formation and its elastic characteristics have a good connection. Shear modulus, bulk modulus, Lame's constant, and Poisson's ratio are most often used modules, where shear modulus is resistance of rock to shear deformation, or in other words, the resistance to deform by parallel force (Figure 2b). As a result of the fact that fluids cannot shear whereas solids can, we may deduce that shear modulus is an excellent indicator of rock matrix. Reluctance of rock to compress or resist volume change is known as bulk modulus or incompressibility. Lame's constant may be calculated using bulk modulus and shear modulus.

$$\lambda = K - 2 * \frac{\mu}{3} \quad (7)$$

The dynamic mechanical properties like Young's Modulus; Bulk Modulus; Rigidity Modulus; and Poisson's Ratio were calculated by using measured wave velocities (Vp and Vs) as follow:

Poisson's Ratio (σ)

Transverse (lateral) strain (extension) to longitudinal strain (contraction) ratio, or the geometrical variation in form of an elastic body, is known as Poisson's ratio. When a solid material is compressed uniaxially, it shortens in the direction of the applied stress and lengthens in the opposite direction.

+ ϵ1: positive elongation, - ϵ3: negative elongation.

$$\sigma = \frac{\epsilon_1}{-\epsilon_3} = \frac{1 - \left(2 * \frac{V_S^2}{V_P^2}\right)}{2 * \left(1 - \frac{V_S^2}{V_P^2}\right)} = \frac{\left(0.5 * \left(\frac{V_P}{V_S}\right)^2\right) - 1}{\left(\frac{V_P}{V_S}\right)^2 - 1}, \quad (8)$$

Poisson's ratio is ranged from 0.5 in fluids and 0.25 in solids, whilst weak materials have values greater than 0.45.

Young Modulus (E)

Burger, 1992 stated that the linear relation between the applied stress (Q) and the resulting strain (ϵ) if a material is subjected to uniaxial compression or tension can be calculated by the relation:

$$\mathbf{Q} = \mathbf{E} * \boldsymbol{\epsilon}, \quad (9)$$

where, the constant E is Young's modulus, (dyne/cm2).

Young's modulus can also be calculated using the equation below.

$$E = \frac{\left(V_S^2 * \rho^3 * \frac{V_P}{V_S}\right) - 4}{\left(\frac{V_P}{V_S}\right)^2 - 1}, \quad (10)$$

VP: compressional wave velocity, VS: transverse wave velocity, and ρ: bulk density.

Rigidity Modulus (μ)

It is a measure of a material's resistance to change in its shape, rigidity modulus gives information about the rock matrix, and calculated from the following equation [38]:

$$\mu = \frac{E}{2 * (1 + \sigma)}, \qquad (11)$$

$$K = \frac{2 * \mu * (1 + \sigma)}{3 * (1 - 2\sigma)} = \frac{E}{3 * (1 - 2\sigma)} \qquad (12)$$

μ: rigidity modulus (dynes/cm2), E: Young's modulus, and σ: Poisson's ratio

Table 1: Lithologic Column of Gebel Abu Hasswa, western Sinai Peninsula side, Egypt and the selected samples.

Age	Fm.	Lithology	Description
Lower Cretaceous	Malha		Sandstone: yellowish brown, pink, alternated with claystone beds 6 samples.
Permo – Triassic	Qisieb		Sandstone: yellowish, red, white, with gypsiferous kaolinite intercalations.
	Aheimer		Claystone: dark purple, intercalated with siliceous & calcareous sandstone beds 10 samples.
Carboniferous	Abu Durba		Laminated sandstone and claystone: dark brown, red with evaporite and dolomite streaks in some parts 3 samples.
U Ordovician – L Silurian	Naqus		Sandstone: white, coarse, pebbles & gravels intercalated with sands, kaolinitic and highly cross bedded.
Cambro - Ordovician	Araba		Sandstone: yellowish brown, coarse, medium to fine, cross bedded with fine shale streaks 32 sample.
Pre - Cambrian	Basement		Basement rock

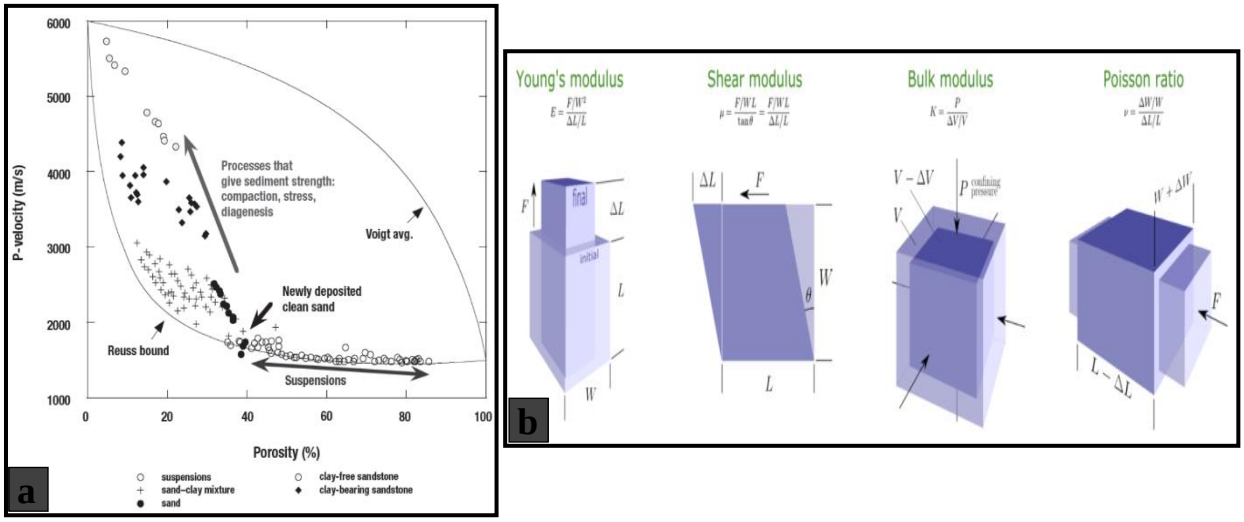

Figure 2: a) P-wave velocity against porosity for a variety of wet sediments, correlated with the Voigt–Reuss bounds. Data are from [35, 36, 37] b) Elastic moduli with stress directions.

Bulk Modulus (K)

When a rock sample is exposed to stress from all directions, it is just the resistance of the rock sample to change in volume. The bulk modulus (K) in (dyne/cm²) is compressive stress divided by the volume change, where the bulk modulus is governed by the kind of fluid if the samples were saturated. Because brine is substantially stiffer than gas, the bulk modulus of brine saturated samples is larger than that of gas saturated samples. The following equation [38] can be used to compute K:

Result

Petrographic investigations

Petrographic investigations of eleven samples selected from Paleozoic Nubia sandstone surface at Gabel Abu Hasswa demonstrates that, all of the samples are composed mainly of sandstone facies classified as quartz arenite (Figure 3). Cementation, dissolution, and compaction are the dominant diagenetic processes; the former is evidenced by silica, calcareous, and ferruginous. The grain contact is indicated by straight and uncommon suture contact. Therefore, this study divided the samples according [39] and depending on the diagenesis processes into (1) Quartz Arenite, (2) Calcareous

Quartz Arenite, (3) Siliceous Quartz Arenite and (4) Ferruginous Quartz Arenite microfacies. Figure 3 represents the prementioned microfacies, where the red circles labeled show the diagenesis process appeared in that slice.

Ray Diffraction Analysis (XRD)

Each sample was powdered to a size of 0.063 mm and quartered, then inspected with a Philips X-ray diffractometer using the Copper tube (Cu). X-ray data were evaluated by using ASTM cards of the data published [40, 41]. Intensity detection was carried out by comparing the strongest lines of the mineral composition of the bulk rock samples. Figure 4 illustrates the relation between the angle of diffraction and intensity of different samples, the identified minerals and intensities show a good correlation with the facies which are classified from the petrographic study. All samples show a high intensity of quartz which proves that all the samples are quartz arenite. In the other hand, the intensity of calcite and kaolinite changes from one sample to another related to the diagenesis processes. Finally, the iron cementation has been revealed as a presence of hematite.

Petrophysical characteristics

Porosity, permeability, and rock density are petrophysical properties, which have been studied to learn more about the acoustic waves of dry samples. This investigation aimed to determine the relationships between both the petrophysical characteristics and the acoustic waves. There are two types of seismic wave velocities propagation: shear and compressional wave velocities (VS and VP). The internal structure, elastic coefficients, and density characteristics of any rock sample influence its ultrasonic wave velocity. The framework of rock, like elastic content of grains, grain density, type of cement, pressure on lithology, and porosity, are summarized as parameters that control rock velocities [6].

Density, porosity, and permeability

Bulk density of Paleozoic rocks of Abu Hasswa section ranged from 1.874 to 2.640 gm/cc, with a mean value 2.09 gm/cc and standard deviation 2.66 gm/cc. Its porosity ranged from 2.69 to 29.6%, with 21.3% mean value and of 5.367% standard deviation. The permeability ranged from 0.0013 to 4027.66 mD, with 877.7 mD mean value, and 1030.02 mD standard deviation.

Porosity and Bulk density relationship

Porosity and bulk density relationship for Araba, Abu Durba, Ahemir, and Malha formations shows an indirect relationship with high correlation coefficients of 0.87 for all the investigated samples, therefore we can calculate porosity from density using the predicted equation (Figure 5a).

Density and Permeability relationship

Figure 5b depicts the relationship between permeability and bulk density for Araba, Abu Durba, Ahemir, and Malha formations. This relationship showed a significant indication for all formations except Araba Formation, where all formations showed that permeability has an indirect relationship with grain density. This could indicate that as the iron oxides percentage increases, it may fill the pore throats, causing permeability to decrease, While Araba Formation may have a different flow unit, causing the relationship to be distorted.

Compressional Velocity (Vp) and Shear Wave Velocity (Vs)

Compressional wave velocity of the study formations of Abu Hasswa section ranged from 1.92 to 4 m/sec, with 2.4 Km/sec mean value and 0.4 m/sec standard deviation, The average values of rocks from the Malha, Ahemir, Abu Durba, and Araba formations are 2.76, 2.26, 3.63, and 2.00 respectively. The shear wave velocity of the same selected samples of Abu Hasswa section ranged from 1.2 to 2.5 m/sec, with 1.6 m/sec mean value, and 0.2 Km/sec standard deviation. Malha, Ahemir, Abu Durba, and Araba formations have mean values of 1.7, 1.59, and 2.00, respectively.

The relationship between petrophysical properties and acoustic wave velocities

Acoustic wave velocities (vp and vs) and bulk density (ρb) relationship

Relationship between the acoustic waves and petrophysical properties has been studied. Figure 6a displays the linear relation between (Vp and Vs) (km/sec) and bulk density (gm/cc) for the study samples. The correlation coefficients for both Vp ,Vs with bulk density are 0.83 and 0.69 respectively. We can see that when the bulk density decreases, Vp and Vs get closer to each other.

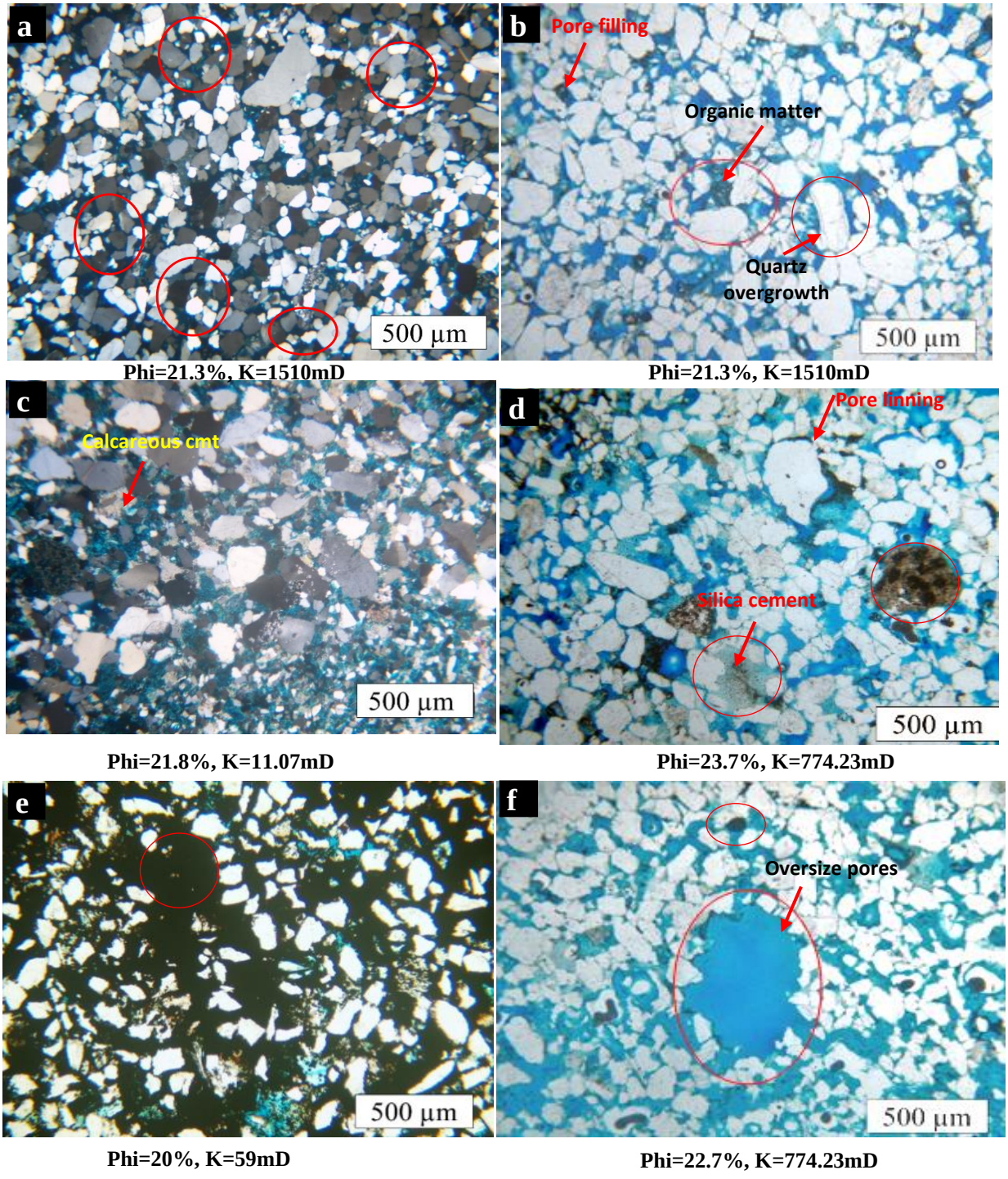

Figure 3: Photomicrographs represent different microfacies; **(a,b)** Quartz Arenite is composed mainly of quartz grains with rare of organic matter and quartz overgrowth, coarse to medium sand size, subangular to subrounded, oversize porosity, moderately sorted, there are different type of contact between grains such as straight, point, concavo- convex and suture contact as shown by red circles photo a. **(c)** Calcareous Quartz Arenite is composed mainly of quartz cemented by calcite, the grains are coarse to fine, subangular to subrounded. **(d)** Siliceous quartz arenite is composed of quartz grains cemented by silica and some carbonate rock fragment (red circles), medium to fine, subangular to subrounded, poorly sorted. **(e)** Ferruginous Quartz Arenite is composed of quartz grains cemented by iron (red circles), fine to medium, subangular to subrounded, moderately sorted. **(f)** Oversize porosity as a result of dissolution processes in addition to pyritization (black spots in red circle).

Acoustic Wave Velocities (Vp and Vs) and Porosity (Ø) relationship

Figure 6b depicts the relation between Acoustic wave velocities and porosity for the selected samples. This relationship revealed an indirect relationship with correlation values of 0.754 for Vp and 0.68 for Vs with porosity.

Compressional Wave Velocity (Vp) and Shear Wave Velocity (Vs) relationship

Figure 6c depicts the relation between Vp and Vs for research samples; this relationship revealed a direct association with an excellent correlation coefficient of 0.75. Figure 6d show the (Vp/Vs) and compressional wave velocity (Vp) relationship for the study samples. This relationship revealed a direct association with a modest correlation coefficient of 0.27 for Vp values.

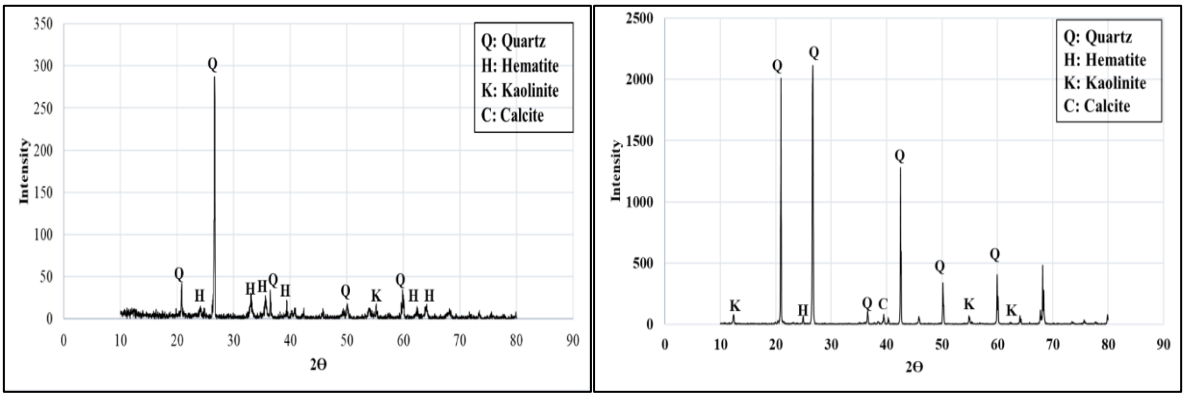

Figure 4: X-ray diffraction cross plot of studied bulk samples.

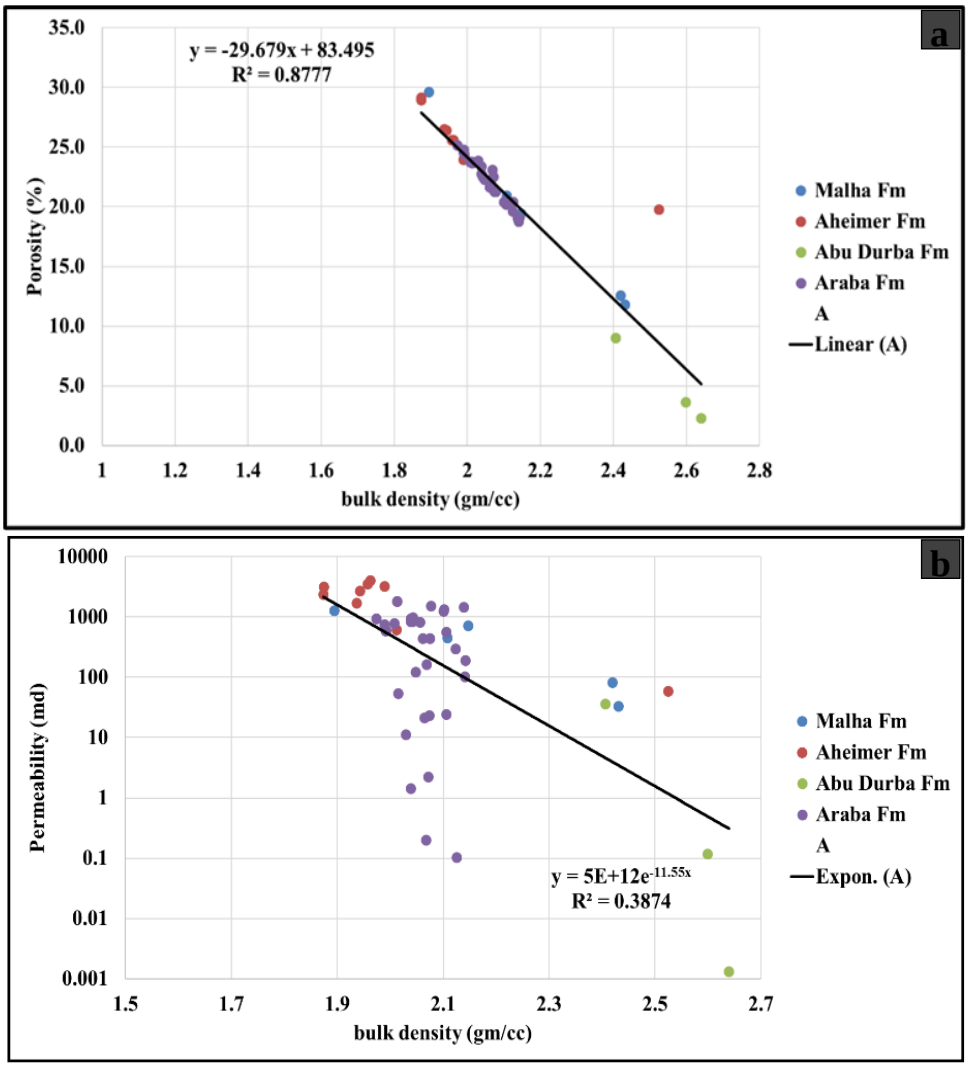

Figure 5: The relationship between a) bulk density and porosity, b) bulk density and permeability.

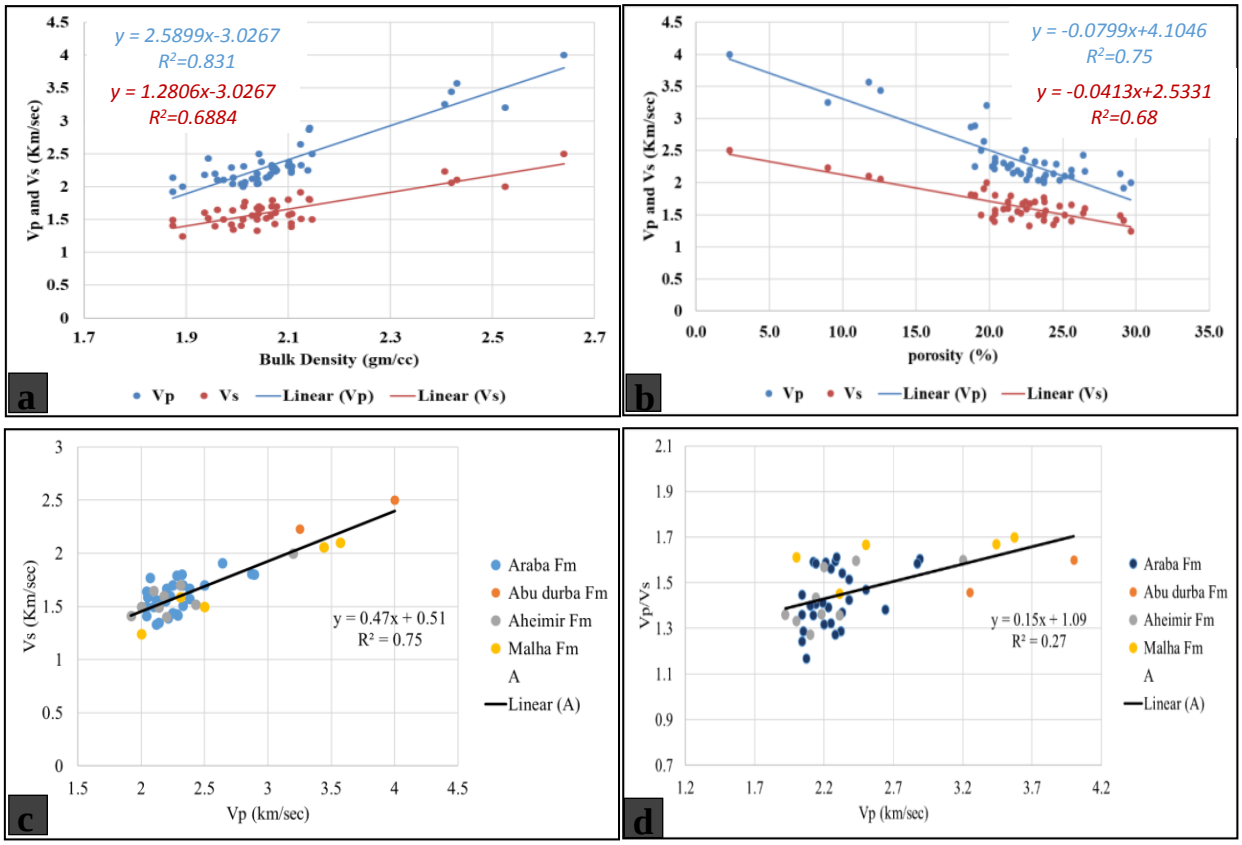

Figure 6: The relationship between a) bulk density and both Vp, Vs; b) porosity and both Vp, Vs; c) Vp and Vs; d) Vp and Vp/Vs.

The relationship between petrophysical parameters and Elastic Moduli

Young's modulus (E) / compressional (Vp) and shear wave (Vs) velocities relationship

Acoustic wave velocities (Vp and Vs) and Young's modulus relationship show a direct relationship with 0.91 and 0.67 correlation coefficients respectively. Regression equations for the acoustic wave velocities and Young's modulus are shown in Figure 7a. These relationships indicate that both Vp and Vs have been affected by Young's modulus, whereas both Vp and Vs increase with increases of Young's modulus.

Rigidity modulus (μ) / compressional (Vp) and shear wave (Vs) velocities relationship

Acoustic wave velocities (Vp and Vs) and rigidity modulus relationship for the study samples revealed a direct relationship with correlation coefficients of 0.75 for Vp and 0.85 for Vs with the regression equations of the acoustic wave velocities and rigidity modulus Figure 7b. This means that both Vp and Vs have been affected by Rigidity modulus, whereas both Vp and Vs increase with increases of Rigidity modulus.

Bulk modulus (K) / compressional (Vp) and shear wave (Vs) velocities relationship

Acoustic wave velocities and bulk modulus relationship for the study materials revealed a direct relationship with correlation values of 0.9 for Vp and 0.48 respectively. The regression equations of the acoustic wave velocities and bulk modulus relationships are shown in Figure 7c. This means that both Vp and Vs have been affected by Bulk modulus, whereas both Vp and Vs increase with increases of Bulk modulus.

Poisson's ratio (σ) and (Vp/Vs) ratio relationship

Dimensionless elastic constant Poisson's ratio (σ) could be used to convert the Vp/Vs ratio. The association between and Vp/Vs ratios is shown in Figure 7d as a direct relationship with a fourth-degree polynomial regression line with a correlation value of R = 0.998. At low Vp/Vs ratios, every tiny change in Vp/Vs will result in huge changes. This means that Poisson's ratio depend strongly upon P-wave velocity, where Poisson's ratio increase with decreases of Vp/Vs ratios.

The relationship between elastic moduli and porosity

Figure 8a depicts the relationship between the multiplication of different elastic moduli in bulk density with porosity for the study samples. This relationship revealed an indirect relationship with correlation coefficients of 0.76 for Lambda*bulk density with porosity and 0.46 for Rigidity* bulk density with porosity, whereas both of them increases with decreases of porosity. The relationship between P-wave velocity and porosity means that P-wave

velocity depends on porosity, where P-wave velocity increases with decreases of porosity.

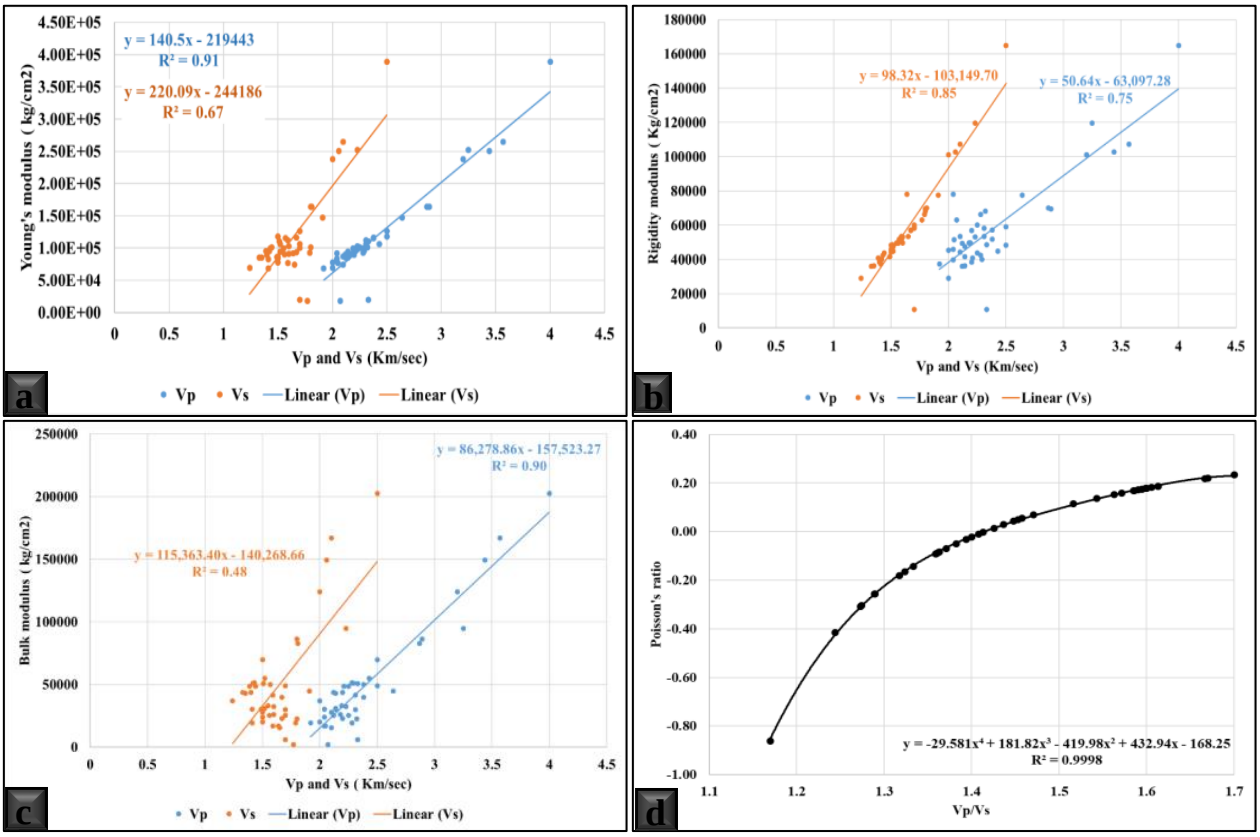

Figure 7: The relationship between a) (Vp and Vs) and (Young's modulus E); b) (Vp and Vs) / (rigidity modulus μ); c) (Vp and Vs) / (bulk modulus K); d) Poisson's ratio (σ) and Vp/Vs ratio.

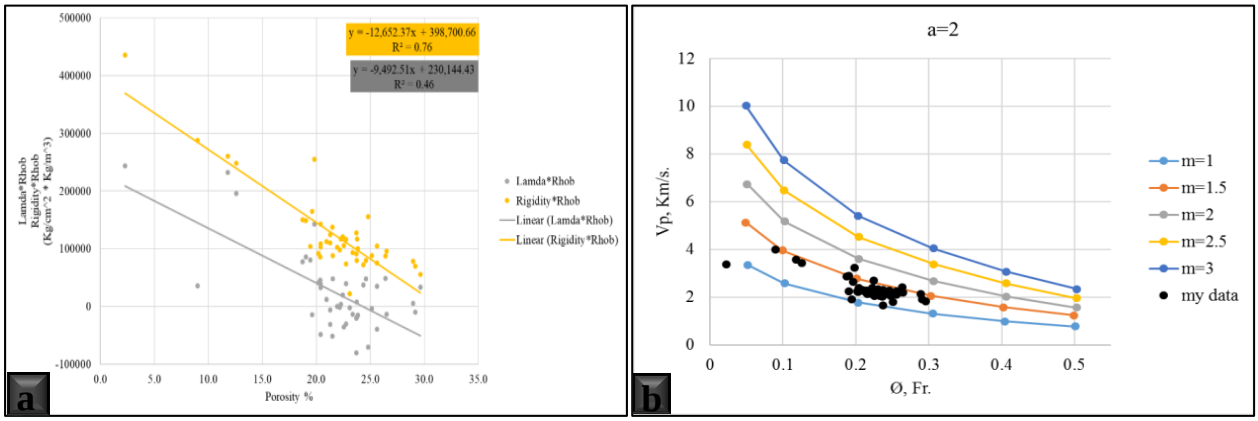

Figure 8: a) The relationship between porosity and (Lambda*Rhob) (Rigidity*Rhob); b) Velocity- porosity Abu Hasswa Section.

Velocity-Porosity Chart for Cementation Exponent Prediction

El-Sayed, (1995) constructed an empirical chart among the compressional velocity (Vp), cementation exponent (m) and porosity (ø), based on an empirical relation between the compressional velocity and f (formation resistivity factor) for a number of surface samples obtained from G. Nazzazat in the western central Sinai. He constructed four charts depending on the multiplier (a) of the general Archie's equation with values of 0.5, 1, 1.5, and 2. This study used El-Sayed chart when the multiplier (a) equals 2.

The cementation was designated to be ranged from 1 up to 3 through the four charts.

Figure 8b illustrates that the study samples of Abu Hasswa section (black dotes) have cementation exponent (m) ranged from 1 to 1.7, which is confirmed with the results of resistivity measurements and electrical flow units' calculations.

$$lnf = 0.9V_p - 0.69, \qquad (13)$$

Discussions

Thin sections description and physical measurement correlation revealed the effect of diagenetic processes on the reservoir quality such as samples characterized by high pore-filling, and pore-lining (Figure 3b,d), in addition to porosity-reducing processes; high cementation with iron oxides and calcareous (Figure 3c,e), in addition to silica overgrowth and the microcrystalline silica (Figure 3b,d), as well as the fine-grained poorly sorted sands and compaction. The cleaned, coarse-grains and well-sorted sands, in addition to porosity-enhancing processes (dissolution and leaching represented in oversized porosity (Figure 3f).

The measured compressional velocity plotted versus to the porosity of some selected samples from Nubia sandstone at Gebel Abu Hasswa (Figure 9) and classified according to Voigt-Reuss cross plot, the projection of samples shows that the study samples are located in the zone of sand with clays mixed with some compacted samples. These compacted samples were also defined using the petrography study as iron cemented facies. The rock samples are exhibiting a higher strength in its compaction and grain to grain contact due to cementation materials such as clay bearing and iron bearing samples. The samples show a high degree of heterogeneity represented in samples going to higher compressional velocity and low porosity.

According to the calculated elastic moduli and the investigation of its relationships with the measured petrophysical properties, the study samples are ranged from highly to moderately compacted samples. The elasticity behaviour of the studied samples can be explained in the light of Poisson's ratio. Samples of high Poisson's ratio are samples that exhibits a bi-directional lateral and axial forces lower than unidirectional force. The most significant feature can be extracted from Poisson's ratio relationship is negative values for many studied samples. The Poisson's ratio negative value is sensitized to the positive axial strain as well as the transvers strain which would proportion directly with cross sectional area. The studied samples of negative Poisson's ratio can be classified as auxetic materials, which become thicker perpendicular to the applied force when stretched.

Vertical profiles of measured petrophysical parameters

The vertical profiling of different measured parameters illustrates the significant markers and differentiate between good and bad quality sandstone. Plots of storage and flow capacity, bulk density and grain density are shown in Figure 10 (a). Changes in porosity and permeability within research samples can be used to determine the quality of sandstone from the Abu Hasswa area. Because of the diagenetic process depicted in cementation, compaction, and dissolution, certain intervals have altered in permeability with no change in porosity and vice versa. The grain qualities and varied textural patterns are also important. All sandstone samples characterized by high porosity and permeability values, except to Abu Durba Formation and lower part of Araba Formation that have a very high concentration of iron oxides where it increases the density of the study samples, in addition to, pore filling with silica and calcareous cement (Figure 10a).

Vertical profiles of measured acoustic and mechanical parameters

Figure (10b) shows the vertical acoustic and mechanical profile of Abu Hasswa section. Acoustic properties mainly affected by compaction, cementation and mineral composition of the samples. It's clearly obvious, Abu Durba Formation is a clear marker of high acoustic properties due to the very low porosity presence, while the other formations have low acoustic properties due to low porosity presence. Where the lower part of Araba Formation has a significant change on the vertical log of Poisson's ratio, lame's constant, and in addition to shear modulus, which can be integrated with the thin section description results that showed pore filling with carbonate and silica overgrowth. Where the mean value of the Poisson's ratio, Lame's constant, and shear modulus within the lower part of Araba Formation is -0.3, -25000, and 30000 (Kg/cm2) respectively.

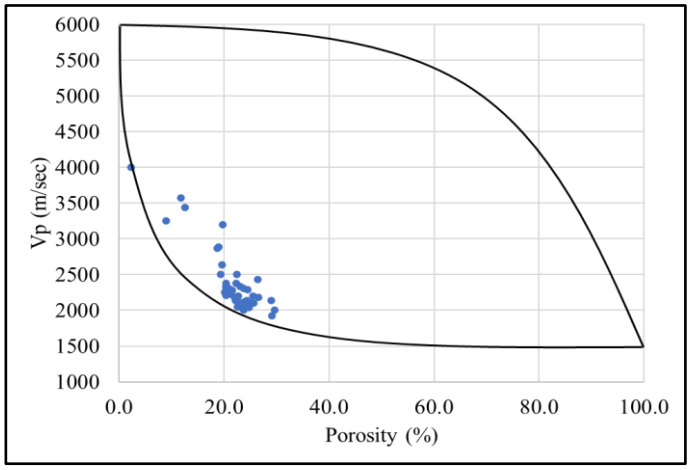

Figure 9: The relationship between Vp and porosity (Voigt-Reuss cross plot).

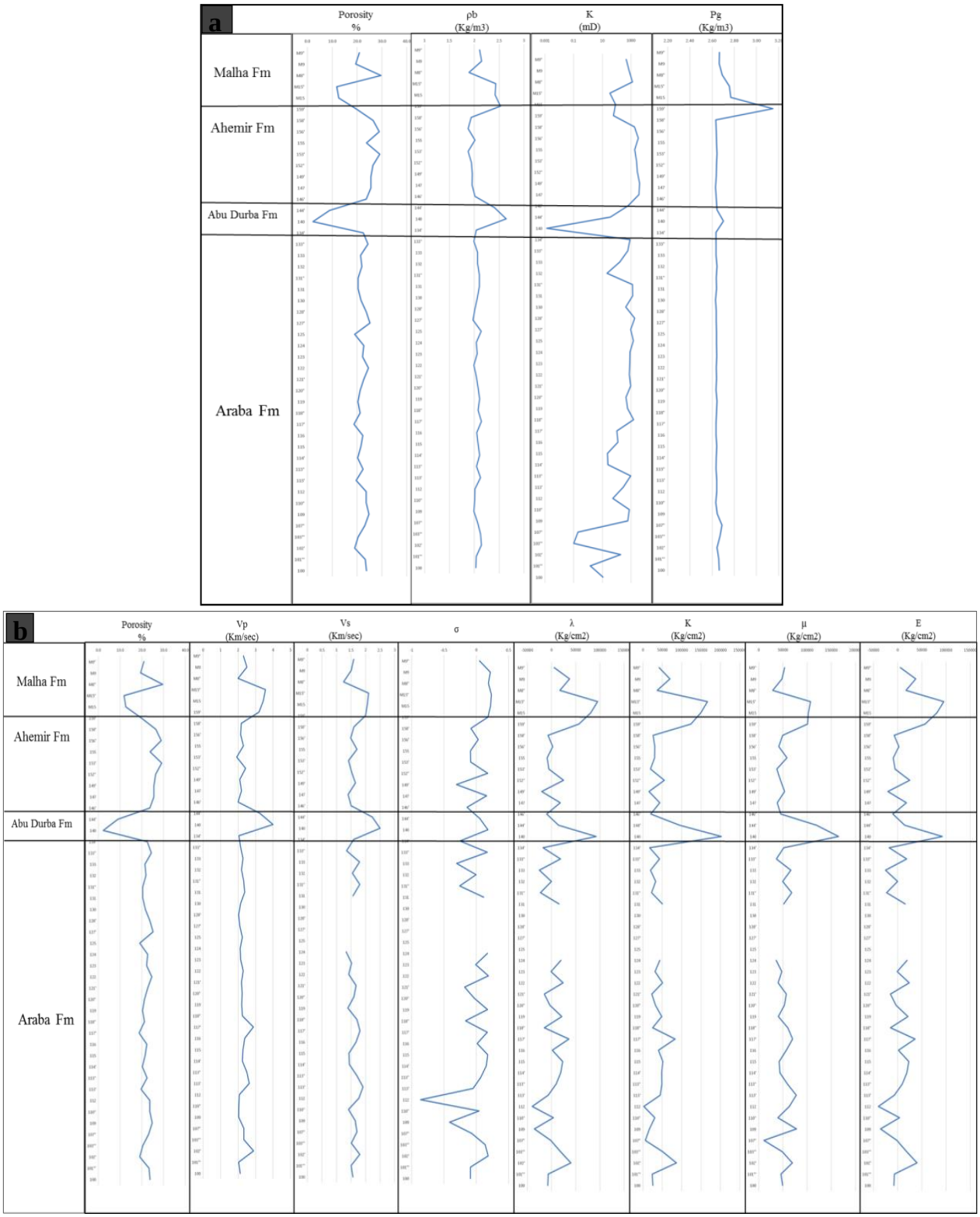

Figure 10: a) Vertical petrophysical profile of Abu Hasswa section; b) Vertical acoustic properties profile of Abu Hasswa section.

Conclusions

The petrophysical evaluation of porosity and permeability of Nubia sandstone samples were carried out for storage and flow capacity assessment, and to detect the degree of heterogeneity. Abu Hasswa section illustrates the relationships with different petrophysical characteristics such as rock density, porosity and permeability; and their effects on the different elastic moduli such as bulk, rigidity, and Young's modulus in addition to lame's constant and Poisson's ratio. Nubia sandstone samples reflect good storage and flow capacity properties at some intervals, while in other some intervals show fair to bad storage and flow capacity properties. This is due to the heterogeneity degree of the study samples that

can be controlled by the sedimentological and diagenetic processes.

The compressional and shear waves have a direct relationship with the bulk density of rocks, which is based on porosity and cementation (silica, calcareous and iron oxides) content. High correlation coefficients were found in the relationships between acoustic waves and porosity and bulk density. Several relationships were carried out as a combination between the different elastic moduli, porosity, bulk density and acoustic velocities. These relationships can prove the lithology of the samples as sandstone and the high correlation coefficients make them very useful for parameters prediction from the others.

The correlation between the different petrophysical parameters like porosity, permeability, grain density, resistivity, and also compressional, and shear wave velocities was carried out using the multi-regression algorithm. The modeled petrophysical parameters showed a significant empirical equation with good to excellent correlation coefficients. The compressional and shear wave velocities show a well correlated indirect relationships with porosity of the rock samples, moreover they were used to calculate the slowness, and Vp/Vs ratio and studied the relationships with different petrophysical parameters. The elastic parameters revealed that there is a significant relationship to the nature of rocks and the diagenesis processes of the study samples, especially the poisons ratio, where the regretted curve was started from 1.17 m/sec and -0.86 which indicate the high degree of diagenesis processes.

Finally, the change in the petrophysical parameters vertically and its relationship with the rock quality show that all sandstone samples are of high porosity and permeability values, except to Abu Durba Formation and lower part of Araba Formation that have high acoustic due to the very low porosity in addition to high concentration of iron oxides where it increases the density of the study samples, in addition to, pore filling with silica and calcareous cement.

Funding sources

On behalf of all authors, the corresponding author states that there is no conflict of interest and we have not received any funding support.

Declarations

Conflict of interest

The authors declare that they have no competing interests.

Acknowledgements

The authors wish to express their thanks and gratitude to the Faculty of science- Ain Shams University and Egyptian Petroleum research institute for permission and release the data for this research.

References

[1] M. Khalifa, H. Soliman, H.A. Wanas, The Cambrian Araba formation in northeastern Egypt: facies and depositional environments. Journal of Asian Earth Sciences, 27, 2006, pp. 873-884.

[2] A.S. Al Sharhan, Petroleum geology and potential hydrocarbon plays in the Gulf of Suez rift basin, Egypt. Rev. AAPG Bull 87 (1), 2003, pp. 143–180.

[3] I. Attia, I. Helal, A. El Dakhakhny, S. Aly, Using sequence stratigraphic approaches in a highly tectonic area: case study – Nubia (A) sandstone in southwestern Gulf of Suez, Egypt. J. Afr. Earth Sci. 2017, (136), 10–21.

[4] M.A. Kassab, M.A. Teama, Hydraulic flow unit and facies analysis integrated study for reservoir characterization: a case study of Middle Jurassic rocks at Khashm El- Galala, Gulf of Suez, Egypt. Arabian J. Geosci. 2018, 11, 294.

[5] M.A. Teama, A.A. Abuhagaza, M.A. Kassab, Integrated petrographical and petrophysical studies for reservoir characterisation of the Middle Jurassic rocks at Ras El-Abd, Gulf of Suez, Egypt. Journal of African Earth Sciences, 152: 2019, 36-47.

[6] W.J. Hicks, J.E. Berry, Application of continuous velocity logs to determination of fluid saturation of reservoir rocks: Geoph., v. 21, no. 3, 1956, p. 739.

[7] B.U. Haq, Jurassic sea-level variations: a reappraisal. GSA Today 28, 2018, 4–10

[8] H. Brandt, A study of the speed of sound in porous granular media. ASME J. Appl. Mech. 22, 1955, 479–486.

[9] M.J. Minear, Presented at the 57th Ann. Mtg. Am. Inst. Min. Metall. Eng., New Orleans, 1982.

[10] A.A. El-Sayed, N.A. El-Sayed, H.A. Ali, M.A. Kassab, S.M. Abdel-Wahab, M.M. Gomaa, () Rock typing based on hydraulic and electric flow units for reservoir characterization of Nubia Sandstone, southwest Sinai, Egypt. Journal of Petroleum Exploration and ProductionTechnology, 2021, https://doi.org/10.1007/s13202-021-01242-x.

[11] M.A. Biot, Theory of propagation of elastic waves in a fluid saturation porous solid II: high frequency range. J. Acoust. Soc. Am. 28, 1956, 179–191.

[12] G. Schweinfurth, Sur la decouverte d unefaunepaleozoiquedans les gres d Egypte. Egyptian Desert Institute Bulletin, 6, 1885, pp. 239-255.

[13] H. Braumann, Note on a geologic reconnaissance made in Arabic Perbraea in the spring of 1868: Quart. J.Geol. Soc. London, v.25, 1869, 17-38.

[14] G.E. Brown, The X-ray identification and crystal structure of clay mineral. Min.Soc. London, 1961, p. 544.

[15] S Omara, Early carboniferous tabulate corals from Um Bogma area, South Western Sinai, Egypt. Riv. Ital. Paleont., v. 77-2, 1971 ,141-154.

[16] B. Issawi, M. Hassan, S. Attia, Geology of Abu Tartur Plateau, Western Desert, Egypt. Annals of the Geological Survey of Egypt, 8 (1978), pp. 91-127.

[17] B. Issawi, M. Hinnawi, L. El khawaga, S. Labib, N. Anany, Contributions to the geology of Wadi Feran

area, Sinai, Egypt" Geol. Surv. Egypt (internal report) 1981, p.43.

[18] B. Issawi, U. Jux, Contributions to the stratigraphy of the Palaeozoic rocks in Egypt. Geological Survey, Egypt, 64, 1982, p. 28.

[19] U. Jux, B. Issawi, Cratonic sedimentation in Egypt during Paleozoic", Annals of the Geological Survey of Egypt, 13, 1983, pp. 223-245.

[20] E. Klitzsch, A. Lejal-Nicol, Flora and fauna from a strata in southern Egypt and northern Sudan (Nubia and surrounding areas). Berliner Geowissenschaftiche Abhandlungen, 50(A), 1984, pp. 47-49.

[21] E. Klitzsch, M. Groschke, W. Hermann-Degen, WadiQena: Paleozoic and pre-Campanian. R. Said (Ed.), The Geology of Egypt, Balkema/Rotterdam/Brookfield, 1990, pp. 321-327.

[22] A.M. Abdallah, M. Darwish, M. El Aref, A.A. Helba, Lithostratigraphy of the pre-Cenomanian clastics of north Wadi Qena, Eastern Desert, Egypt. A. Sadek (Ed.), Proceedings of the First International Conference on Geology of the Arab World, Cairo University, Cairo 1992, pp. 255-282.

[23] R. Said The geology of Egypt. Elsevier publishing Company, Amsterdam, New York, 1962,P. 1 – 277.

[24] M.G. Barakat, General Review of the Petroliferous Provinces of Egypt. Petroleum and Gas Project, Cairo Univ. /M.I.T. Technology Planning Program, 1982.

[25] M. El-Beleity, M. Ghoneim, M. Hinawi, M. Fathi, G. Gebali, M. Kamal, Paleozoic stratigraphy, and paleotectonics in the Gulf of Suez. 8th EGPC Conference, Cairo. 1. 21, 1986.

[26] M.W. El-Dakkak, Geological studies of subsurface Paleozoic strata of northern Western Desert, Egypt. Journal of African Earth Sciences, 7 1988, pp. 103-111.

[27] M.L. Keeley, The Paleozoic history of the Western Desert of Egypt. Basin Research, 2 , 1989, pp. 35-48.

[28] M.A. Kora, Lithostratigraphy of the Early Paleozoic succession in Ras El-Naqab area, east-central Sinai, Egypt. Newsletters Stratigraphy, 24, 1991, pp. 45-55.

[29] H.M. Khalil, Geology of the area between Wadi Feiran and El-Tor, south west Sinai, Egypt. M.Sc. Thesis, Tanta University, 1987, 130p.

[30] J.W. Amyx, D.M. Bass, R.L. Whiting, Petroleum reservoir engineering. McGraw Hill Publ. Co., New York, NY, 1960, p. 601.

[31] M.R.J. Wyllie, A.R. Gregory, L.W. Gardnet, An experimental investigation of factors effecting elastic wave velocities in porous media. Geophysics 23, 1958, 450–493.

[32] A. Salah, Effects of Fluids Saturation on the Acoustic Properties of the Upper Cretaceous Reservoirs, Western Desert, Egypt. M.Sc,Thesis, Ain Shams University, 2001, pp. 175.

[33] M.A. Kassab, The behavior of acoustic wave velocity in some Paleozoic sandstone samples. Petrol. Sci. Technol. 29, 2011, 260–270.

[34] M.A. Kassab, A. Weller, Study on P-wave and S-wave velocity in dry and wet sandstones of Tushka region, Egypt. Egypt. J. Petrol. 24, 2015, 1–11.

[35] H. Yin, Acoustic velocity and attenuation of rocks: Isotropy, intrinsic anisotropy, and stress induced anisotropy, 1992.

[36] D.H. Han, Effects of porosity and clay content on acoustic properties of sandstones and consolidated sediments. Ph.D. Thesis, Stanford University, 1986.

[37] E.L. Hamilton, Low sound velocities in high porosity sediments. Acoustical Soc. Am., 28: 1956, 16-19.

[38] H. Burger, Exploration geophysics of the shallow subsurface: Englewood Cliffs, N.J., Prentice-Hall, 1992, 489 p.

[39] R.L. Folk (): Some aspects of recrystallization in the ancient limestones. In Pray and Murray (Ed.), Dolomitization and limestone diagenesis. Soc. Econ. Paleant, Miner, Sp. Pub., V. 13, 1965, p. 14-48.

[40] T. Barron, The topography and geology of the peninsula of Sinai (western portion). Survey Dept., Cairo, 1907, pp. 241.

[41] D.M. Moore, J.r. R.C. Reynolds, X-ray diffraction and the identification and analysis of clay minerals, 2nd edn. Oxford. University Press, Oxford, 1997, p. 378.